Quenching of exciton luminescence in SrF_2 nanoparticles within a diffusion model

M. Chylii, T. Demkiv, V. Vistovskyy, T. Malyi, A. Vasil'ev, and A. Voloshinovskii

Citation: Journal of Applied Physics **123**, 034306 (2018);
View online: https://doi.org/10.1063/1.5005621
View Table of Contents: http://aip.scitation.org/toc/jap/123/3
Published by the American Institute of Physics

Articles you may be interested in

Addressing limitations of photoluminescence based external quantum efficiency measurements
Journal of Applied Physics **123**, 023105 (2018); 10.1063/1.5004193

Pressure, temperature, and thickness dependence of transmittance in a 1D superconductor-semiconductor photonic crystal
Journal of Applied Physics **123**, 033101 (2018); 10.1063/1.5009708

Linear and nonlinear magneto-optical properties of monolayer MoS_2
Journal of Applied Physics **123**, 034301 (2018); 10.1063/1.5009481

Analytical modelling for predicting the sound field of planar acoustic metasurface
Journal of Applied Physics **123**, 033106 (2018); 10.1063/1.5000055

Vortex-chirality-dependent standing spin-wave modes in soft magnetic nanotubes
Journal of Applied Physics **123**, 033901 (2018); 10.1063/1.5010405

Compositional and strain analysis of In(Ga)N/GaN short period superlattices
Journal of Applied Physics **123**, 024304 (2018); 10.1063/1.5009060

Quenching of exciton luminescence in SrF_2 nanoparticles within a diffusion model

M. Chylii,[1] T. Demkiv,[1] V. Vistovskyy,[1] T. Malyi,[1] A. Vasil'ev,[2] and A. Voloshinovskii[1]
[1]*Ivan Franko National University of Lviv, 8 Kyryla i Mefodiya, 79005 Lviv, Ukraine*
[2]*Skobeltsyn Institute of Nuclear Physics, Lomonosov Moscow State University, 119991 Moscow, Russian Federation*

(Received 19 September 2017; accepted 3 January 2018; published online 18 January 2018)

Quenching processes of the self-trapped exciton luminescence were studied analyzing the shape of X-ray luminescence decay kinetics curves of SrF_2 nanoparticles of different sizes. To describe the curves of luminescence decay kinetics, an equation was obtained which is based on the model which takes into account the diffusion of self-trapped excitons and which considers the case of strong surface quenching. The obtained relation was shown to describe the shape of the experimental curves of X-ray luminescence decay kinetics of SrF_2 nanoparticles if their size distribution is bi-modal, i.e., a log-normal distribution about a mean size in the tens of nanometers range plus a distribution of particles larger than 130 nm. The presence of large particles is implied in this model by the single-exponential decay with time constant of 1.2 μs. From the fitting of kinetics curves using the proposed relation, the average diffusion length of self-trapped excitons in SrF_2 was estimated to be (15 $\pm$ 2) nm. *Published by AIP Publishing*. https://doi.org/10.1063/1.5005621

I. INTRODUCTION

Presently, the effect of nanoparticle sizes on their luminescence intensity is being deeply studied for the cases of impurity and intrinsic luminescence.[1–6] In the case of the intracenter excitation, the luminescence intensity decreases with a decrease in the nanoparticles size. In small-sized nanoparticles, it is explained by the growing influence of surface effect, which leads to non-radiative relaxation of excited luminescence centers due to the interaction with surface defects.[1] When the luminescence is excited by the photons in the region of band-to-band absorption transitions or by X-ray quanta, in addition to quenching, resulting from interaction of excited centers with quenching centers, the decrease in the luminescence intensity due to excitation energy losses during migration of free charge carriers is observed. It was shown for a number of nanoparticles possessing both the intrinsic and the impurity luminescence,[2–5] including SrF_2.[6]

Besides the intensity decrease with a decrease in the size of the nanoparticles, the shape of luminescence decay kinetics curve changes as well.[6–8] In the luminescence decay kinetics of nanoparticles, a "fast component" appears and its relative contribution increases with the nanoparticle size decreasing. The appearance of the "fast component" is associated with the processes of non-radiative relaxation of luminescence centers caused by the interaction with surface defects. The processes of non-radiative relaxation of self-trapped excitons (STE) due to the interaction with the surface defects in SrF_2 nanoparticles can be studied properly using an X-ray excitation, since the luminescence decay time measurements in the case of direct optical formation of excitons require excitation with photon energies in the vacuum ultraviolet (VUV) range ($h\nu \approx 10.2$ eV).

In this paper, the variation of the shape of X-ray luminescence decay kinetics in SrF_2 nanoparticles depending on their sizes is analyzed. For this purpose, a model for exciton luminescence decay including the influence of exciton diffusion has been developed, assuming that non-radiative exciton relaxation occurs when the latter are located on the nanoparticle surface. A similar approach has also been used for bulk materials, where the deviation of the shape of luminescence decay kinetics from exponential one is explained by the migration of the excitation to the near-surface region within the frames of semi-infinite space ($x > 0$) model representing a crystal.[9]

II. EXPERIMENT

The luminescence properties of SrF_2 different-sized nanoparticles obtained by the method described in Ref. 6 are analyzed. The average size of the nanoparticles obtained as a result of synthesis by the co-precipitation method is 20 nm. The nanoparticle samples with larger average sizes were obtained by annealing at various temperatures. The average sizes of investigated nanoparticles of 20, 30, 45, 65, and 85 nm were determined by the broadening of diffraction peaks.[6]

Measuring the luminescence spectra and luminescence decay kinetics of SrF_2 nanoparticles upon pulse X-ray excitation was carried out using the facility based on the LOMO MDR-2 monochromator. The facility allows to carry out the luminescence-kinetic measurements in a time range of 10^{-9}–10^{-6} s in the 200–800 nm spectral region. The anode voltage of the X-ray tube was equal to 40 kV, the average current—100 mA, and the pulse duration—2 ns.[3] The average energy of X-ray quanta was about 20 keV. The attenuation length of such X-ray quanta for SrF_2 is about 77 μm, which is considerably less than the thickness (2 mm) of the studied powder nanoparticle samples.

Luminescence studies of SrF_2 nanocrystals upon photoexcitation were performed in SUPERLUMI station at HASYLAB (DESY, Hamburg).[10]

III. EXPERIMENTAL RESULTS

The SrF_2 nanoparticles excited by the synchrotron radiation quanta in the region of optical exciton formation ($h\nu = 10.2$ eV) reveal luminescence spectra (Fig. 1, curves 1, 2) similar to the spectra of their bulk analogues.[11–13] The spectra consist of asymmetric emission band with a maximum peaked at $\lambda = 305$ nm (4.06 eV). Measurements of the luminescence spectra with time resolution at room temperature show that only a slow decay component of microsecond range is present. The luminescence is identified as π-component of self-trapped exciton emission.[11]

The photoluminescence intensity of nanoparticles becomes approximately 5 times lower as the nanoparticle size decreases from 85 to 20 nm (Fig. 1, curves 1, 2, and 5). The intensity of exciton luminescence decreases in this case due to the quenching as a result of interaction with the near-surface defects, whose role increases with nanoparticle sizes decreasing.

As can be seen from the normalized luminescence excitation spectra (Fig. 1, curves 3, 4), the luminescence intensity decrease with a decrease in the nanoparticle sizes varies for different excitation energies. Thus, under direct optical formation of excitons ($h\nu_{exc} = 10.2$ eV), the intensity decrease rate with decreasing nanoparticle sizes is much less than the one in the case of excitation in the band-to-band absorption region [$h\nu_{exc} > E_g = 11.3$ eV (Ref. 14)]. The latter can be explained by the STE luminescence quenching due to the interaction with surface defects combined with an additional quenching mechanism caused by the excitation energy losses at the stage of free charge carrier migration ($h\nu_{exc} > E_g$). Since the thermalization length becomes comparable to the size of the nanoparticles, free charge carriers reach the nanoparticle surface without exciton formation.[2–6] The same considerations can explain a more pronounced decrease in the luminescence intensity of SrF_2 nanoparticles with the decrease in their sizes observed in the case of X-ray excitation as compared with that under optical excitation (Fig. 1, curves 5 and 6).

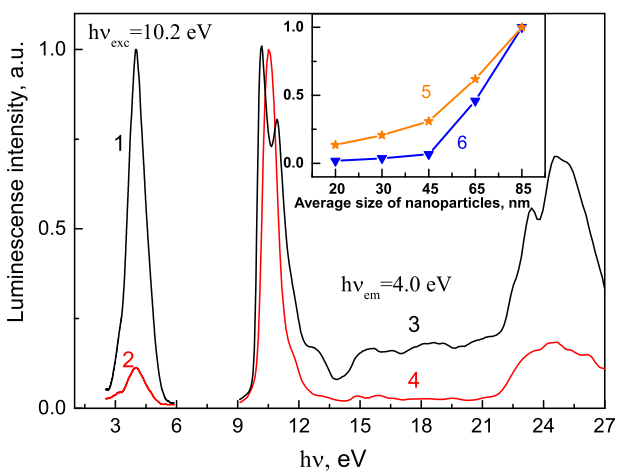

FIG. 1. Emission (curves 1, 2) and luminescence excitation (3, 4) spectra of SrF_2 nanoparticles with mean grain size of $a_0 = 85$ nm (1, 3) and $a_0 = 20$ nm (2, 4) at 300 K. Emission spectra measured at the same conditions reflect the difference in the luminescence intensity for nanoparticles of different sizes. The luminescence excitation spectra are normalized. Inset: the comparison of luminescence intensity dependence on the nanoparticle sizes upon photo- (curve 5, $h\nu_{exc} = 10.2$ eV) and X-ray excitation (6). $T = 300$ K.

The luminescence quenching at the stage of free charge carrier migration should not affect the exciton luminescence decay kinetics, since these losses of excitation energy take place before the formation of excitons. Therefore, the change of X-ray luminescence decay kinetics with nanoparticle sizes decreasing can be considered as a consequence of quenching of excitons due to their interaction with the near-surface defects.

X-ray excited STE luminescence decay kinetics for the single crystal and SrF_2 nanoparticles with different sizes are shown in Fig. 2. The decay kinetics curve of the single crystal (curve 1) is close to the exponent with the decay time constant $\tau = 1.2\ \mu$s. The exponential form and fast luminescence rise suggest that the X-ray excited luminescence decay kinetics of SrF_2 is not distorted by the capture of charge carriers by traps during their migration. The insignificant deviation of X-ray-luminescence kinetics of the SrF_2 single crystal (curve 1) from the exponential form at the initial stage of the decay is possibly due to the presence of defects or uncontrolled impurities in the crystal, resulting in the quenching of the exciton luminescence.

X-ray STE luminescence decay kinetics in SrF_2 nanoparticles (Fig. 2, curves 2–6) in addition to the exponential component, which corresponds to the exciton decay time at room temperature, exhibits pronounced fast component and its contribution increases with a decrease in the nanoparticle sizes. We suggest that this fast component appears due to the quenching of STE involving near-surface defects. To analyze the decay kinetics of X-ray STE luminescence in nanoparticles, a model taking into account the diffusion of excitons toward the surface was developed.

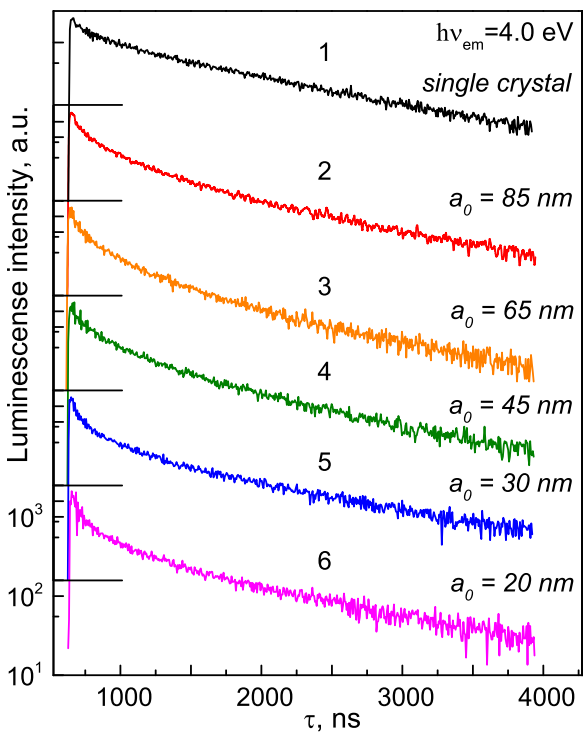

FIG. 2. X-ray excited luminescence decay kinetics of SrF_2 single crystal (curve 1) and nanoparticles of different average grain sizes (2–6). $T = 300$ K.

IV. KINETICS FOR SURFACE LOSSES IN NANOPARTICLES

For simplicity, we regard a nanoparticle as a rectangular parallelepiped with the length of edges equal to a_x, a_y, and a_z, correspondingly: $0 < x < a_x$, $0 < y < a_y$, $0 < z < a_z$. The excitation light falls along the x-axis. The concentration of excitons (probability density of finding an exciton) is denoted as $n(t, x, y, z)$. After the instant excitation with the light intensity of I_{ex} photons per unit square, this concentration is controlled by the equation

$$\frac{\partial n(t,x,y,z)}{\partial t} = D\left(\frac{\partial^2 n}{\partial x^2} + \frac{\partial^2 n}{\partial y^2} + \frac{\partial^2 n}{\partial z^2}\right) - \frac{n}{\tau}, \qquad (1)$$

where D is the exciton diffusion coefficient, and τ is the exciton radiation lifetime. This equation can be easily solved by Laplace transformation over time and Fourier transformation over space coordinates. We are going to discuss the case of strong surface quenching. In this case, excitons are instantaneously killed at the surfaces of the nanoparticles, and the boundary conditions are $n(t, 0, y, z) = n(t, a_x, y, z) = 0$, $n(t, x, 0, z) = n(t, x, a_y, z) = 0$, and $n(t, x, y, 0) = n(t, x, y, a_z) = 0$. Therefore, this model is suitable for nanoparticles and single crystals having a strong nonradiative relaxation of excitons on their surface.

The initial condition is $n(0, x, y, z) = I_{ex}k_{ex}e^{-k_{ex}x}$, where k_{ex} is the absorption coefficient for the excitation light. This condition is suitable for single crystals both in optical and X-ray excitation. In the latter case, k_{ex} is the extinction coefficient of X-ray quanta. In the case of nanocrystals $ak_{ex} \ll 1$, the initial exciton distribution can be considered to be uniform $n(0, x, y, z) = I_{ex}k_{ex} = const$, which is a partial case of the previous initial condition.

Solving the boundary value problem (see the detailed description the in Appendix) for the case of nanoparticles in the form of a cube ($a = a_x = a_y = a_z$) with the size less than the absorption length ($ak_{ex} \ll 1$), one can obtain the following expression for luminescence decay intensity:

$$I_{lum}(t) = I_{lum}(0)\exp\left(-\frac{t}{\tau}\right)\left(R\left(\frac{L^2}{a^2}\frac{t}{\tau}\right)\right)^3, \qquad (2)$$

where

$$R(x) = \frac{8}{\pi^2}\sum_{n=1}^{\infty}\frac{1}{(2n+1)^2}\exp\left(-(2n+1)^2\pi^2 x\right),$$

and L—mean diffusion length of self-trapped excitons.

The luminescence decay kinetic curves constructed according to the relation (2) are shown in Fig. 3. As it can be seen from the figure, the increase in the rate of luminescence decay kinetics is observed if diffusion of excitons to the nanoparticle surface is accounted for, especially at the initial stage of luminescence quenching.

V. FITTING THE X-RAY LUMINESCENCE DECAY KINETICS BASED ON THE DIFFUSION MODEL

The fitting parameters in formula (2) are: τ—decay time of STE, L—the mean migration length of STE during time τ,

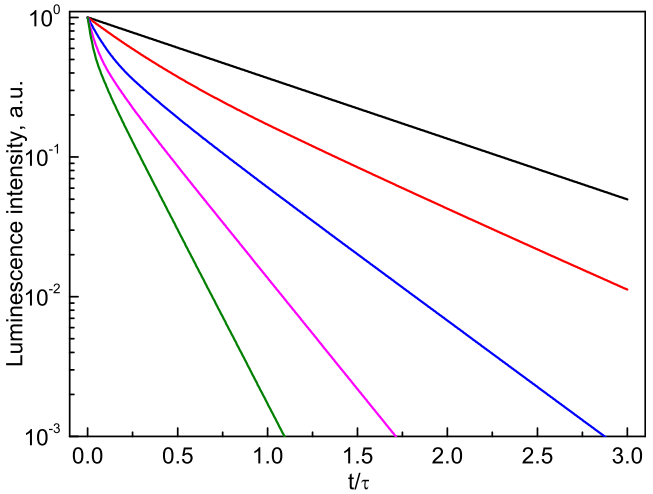

FIG. 3. Decay curves for $L/a = 0$ (upper curve), 0.1, 0.2, 0.3, and 0.4 (bottom curve).

and a_0—nanoparticle size. Experimental curves of X-ray luminescence decay kinetics (Fig. 2) cannot be fitted with Eq. (2) if parameter a_0 takes on the values of experimental average sizes of the nanoparticles (20, 30, 45, 65, and 85 nm). This is caused by the fact that nanoparticles have a certain size distribution. In order to take it into account, we introduce the distribution function of the nanoparticles size $N(a)$. Then, considering the contribution of nanoparticles with different sizes in the test sample, the experimental kinetics curve $I(t)$ would be described by the relation

$$I(t) = \int_0^{a_{\max}} I_{lum}(t, a)N(a)da, \qquad (3)$$

where $I_{lum}(t, a)$ is the decay kinetics for nanoparticles of the same size from relation (2).

As the first step to the analysis of kinetics curves (Fig. 2), Eq. (3) was solved in order to determine the possible form of the function $N(a)$. Equation (3) is Fredholm equation of the first kind. This equation was solved by numerical methods, according to the algorithm described in Ref. 15, substituting the function $I(t)$ by the experimental decay kinetics data. Regularization by Tikhonov method was used in calculations. The mean diffusion length L was chosen from a range of 4–15 nm as it is presented in Refs. 6 and 11. The decay time of the exciton $\tau = 1.2\ \mu s$ was taken from the fitting of the kinetics of SrF_2 single crystal (Fig. 2, curve 1). The function $N(a)$ as a typical solution of the integral equation (3) is shown in Fig. 4.

As can be seen from Fig. 4, the obtained curve $N(a)$ contains the contribution of nanoparticles with sizes $a > 130$ nm in addition to the distribution of nanoparticle sizes in the vicinity of average value (20 nm). This result indicates that the sample contains nanoparticles with the ratio $L/a \ll 1$. Particles with such large sizes have the single-exponential decay kinetics characteristic of SrF_2 single crystals. Therefore, the size distribution is considered only for small nanoparticles, and the presence of large particles is taken into account by adding the one-exponential term in Eq. (3)

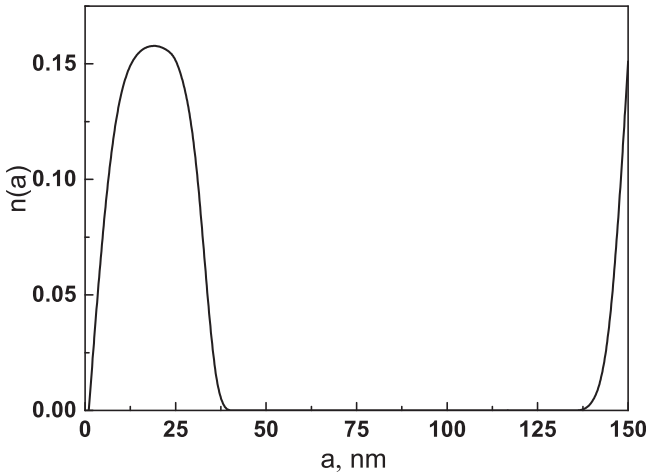

FIG. 4. The size distribution of nanoparticles obtained from the solution of Eq. (3) for the X-ray excited luminescence decay kinetics in SrF_2 nanoparticles of $a_0 = 20$ nm average grain size. $L = 10$ nm.

$$I(t) = (1 - A) \int_0^{a_{\max}} I_{lum}(t, a) N'(a) da + Ae^{-\frac{t}{\tau}}, \qquad (4)$$

where the value of A determines the contribution of luminescence from the large nanoparticles. The log-normal distribution was chosen to fit the experimental kinetics using relation (4) for the size distribution of nanoparticles ($N'(a)$)

$$N'(a) = \frac{1}{\sqrt{2\pi}\, a \ln(\sigma)} \exp\left[-\frac{1}{2} \left(\frac{ln\left(\frac{a}{a_0}\right)}{ln(\sigma)} \right)^2 \right],$$

where a_0 is the average nanoparticle size, σ—parameter that determines the distribution width. The optimal value of $\sigma = 2$ was chosen during the fitting procedure of the decay kinetics. The distribution of nanoparticles with different average sizes is shown in Fig. 5.

Using the distributions shown in Fig. 6 as $N'(a)$ functions and decay time of STE $\tau = 1.2\ \mu$s, the approximations of the experimental luminescence kinetics decay (Fig. 2) were carried out. The mean diffusion length of STE (L) and the contribution to the emission from large nanoparticles (A) were used as fitting parameters. The examples of fits are shown in Fig. 6,

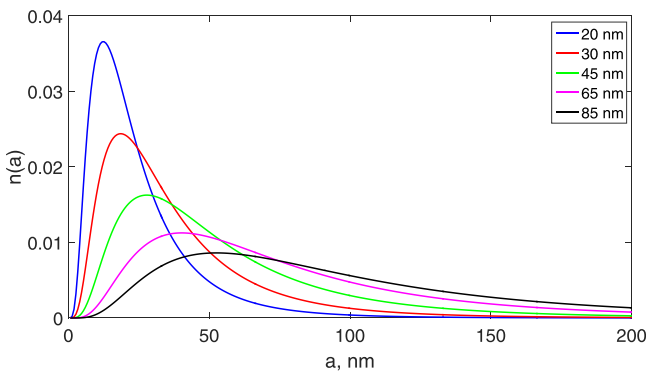

FIG. 5. Log-normal distribution in case $\sigma = 2$ and $a_0 = \{20, 30, 45, 65, \text{and } 85\ \text{nm}\}$.

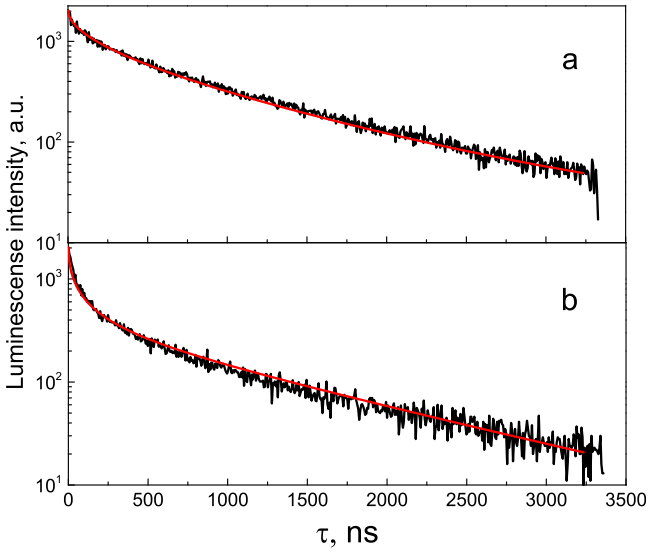

FIG. 6. X-ray excited luminescence decay kinetics of SrF_2 nanoparticles (black curves) and fitting curves (red) using Eq. (4) for samples with the average grain size of $a_0 = 85$ nm (a) and $a_0 = 20$ nm (b).

and the corresponding parameters are given in Table I. The best fits of the experimental data were obtained using the mean diffusion length of STE in the range of 13–17 nm and the relative emission contribution of large nanoparticles of about 10% (Table I).

The proposed model of diffusion quenching of STE luminescence allows one to describe well the experimental curves of exciton luminescence decay kinetics in nanoparticles of different sizes. In addition, the implementation of this model gives an opportunity to determine the particle size distribution or the diffusion length of STE by indirect methods.

VI. CONCLUSIONS

A model of STE luminescence quenching in nanoparticles is proposed taking into account the diffusion processes of STE inside the nanoparticle volume and the interaction with surface defects. Fitting of the experimental curves by the proposed relation that accounts for the nanoparticle size distribution makes it possible to obtain the estimation of the mean diffusion length L of STE. The estimated value of L for SrF_2 is in the range of 13–17 nm. If the value of diffusion length of STE L is known for a certain material, then using this model, the size distribution of nanoparticles can be

TABLE I. Fitting the parameters of X-ray excited luminescence decay kinetics using Eq. (4) for nanoparticles with different average grain sizes. L—the diffusion length of STE; A—the relative contribution in emission intensity from "large" nanoparticles in the samples.

Nanoparticles average size (nm)	L (nm)	A
20	13	0.11
30	14	0.13
45	15	0.13
65	17	0.08
85	17	0.13

calculated by solving the Fredholm integral equations of the first kind.

The proposed model allows us to analyze the kinetics of exciton luminescence in nanoparticles and single crystals that have a strong nonradiative relaxation of excitons on their surface.

ACKNOWLEDGMENTS

The authors are thankful for the support by the Ministry of Education and Science of Ukraine.

Andrey Vasiliev thanks the support by the Ministry of Education and Science of the Russian Federation (state Contract No. RFMEFI61614X0006).

APPENDIX: LUMINESCENCE DECAY KINETICS WITH REGARD TO SURFACE LOSSES

To obtain the expression for luminescence intensity time dependence according to the above-described model (Sec. IV), it is necessary to solve the following boundary value problem:

$$\begin{cases} \dfrac{\partial n(t,x,y,z)}{\partial t} = D\left(\dfrac{\partial^2 n}{\partial x^2}+\dfrac{\partial^2 n}{\partial y^2}+\dfrac{\partial^2 n}{\partial z^2}\right)-\dfrac{n}{\tau} \\ n(0,x,y,z) = I_{ex}k_{ex}e^{-k_{ex}x} \\ n(t,0,y,z) = n(t,a_x,y,z) = 0 \\ n(t,x,0,z) = n(t,x,a_y,z) = 0 \\ n(t,x,y,0) = n(t,x,y,a_z) = 0. \end{cases} \tag{A1}$$

These boundary conditions are satisfied if we take only Fourier terms with wavevector components $k_x = n_x\frac{\pi}{a_x}$, $k_y = n_y\frac{\pi}{a_y}$, and $k_z = n_z\frac{\pi}{a_z}$. It can be shown that terms with even n_x, n_y and n_z disappear after the integration of emission intensity over nanoparticle volume, so significant wavevector components are

$$k_x = (2n_x+1)\frac{\pi}{a_x},\ k_y = (2n_y+1)\frac{\pi}{a_y},\ k_z = (2n_z+1)\frac{\pi}{a_z}. \tag{A2}$$

We can express the initial conditions using equalities

$$1 = \sum_{n=0}^{\infty}\frac{4}{\pi(2n+1)}\sin\left(\pi(2n+1)x/a\right), \tag{A3}$$

$$e^{-kx} = \sum_{n=1}^{\infty}\frac{2n\pi\left(1-e^{-ka}(-1)^n\right)}{a^2k^2+\pi^2n^2}\sin(\pi nx/a). \tag{A4}$$

Each mode with wavevector components from Eq. (A2) will decay with rate

$$\lambda_{n_x,n_y,n_z} = \frac{1}{\tau}+D\left(\frac{(2n_x+1)^2\pi^2}{a_x^2}+\frac{(2n_y+1)^2\pi^2}{a_z^2}+\frac{(2n_z+1)^2\pi^2}{a_y^2}\right). \tag{A5}$$

After some algebraic transformations, one can obtain the intensity of luminescence emitted by the nanoparticle after instantaneous excitation

$$I_{lum}(t) = \frac{256a_xa_ya_z}{\pi^4\tau}(1+e^{-a_xk_{ex}})I_{ex}k_{ex}\sum_{n_x=0}^{\infty}\sum_{n_y=0}^{\infty}\sum_{n_z=0}^{\infty} \times\frac{1}{(a_x^2k_{ex}^2+\pi^2(2n_x+1)^2)(2n_y+1)^2(2n_z+1)^2}e^{-\lambda_{n_x,n_y,n_z}t}. \tag{A6}$$

The amplitude of the luminescence just after excitation can be simplified and it equals to

$$\begin{aligned} I_{lum}(0) &= \frac{256a_xa_ya_z}{\pi^4\tau}(1+e^{-a_xk_{ex}})I_{ex}k_{ex} \\ &\times\left(\sum_{n_x=0}^{\infty}\frac{1}{a_x^2k_{ex}^2+\pi^2(2n_x+1)^2}\right)\left(\sum_{n_z=0}^{\infty}\frac{1}{(2n_z+1)^2}\right)^2 \\ &= \frac{a_ya_z}{\tau}(1-e^{-a_xk_{ex}})I_{ex}. \end{aligned} \tag{A7}$$

This value equals the total number of excitons created in the nanoparticle divided by the radiation lifetime.

The decay kinetics can be rewritten in the form

$$\frac{I_{lum}(t)}{I_{lum}(0)} = \exp\left(-\frac{t}{\tau}\right)P\left(\frac{D\,t}{a_x^2},a_xk_{ex}\right)R\left(\frac{D\,t}{a_y^2}\right)R\left(\frac{D\,t}{a_z^2}\right), \tag{A8}$$

where we introduce two auxiliary functions

$$R(x) = \frac{8}{\pi^2}\sum_{n=1}^{\infty}\frac{1}{(2n+1)^2}\exp\left(-(2n+1)^2\pi^2x\right) \tag{A9}$$

and

$$P(x,y) = 4y\frac{1+e^{-y}}{1-e^{-y}}\sum_{n=1}^{\infty}\frac{1}{y^2+\pi^2(2n+1)^2}\exp\left(-(2n+1)^2\pi^2x\right). \tag{A10}$$

It can be checked that

$$R(0) = \frac{8}{\pi^2}\sum_{n=1}^{\infty}\frac{1}{(2n+1)^2} = 1, \tag{A11}$$

$$\begin{aligned} P(0,y) &= 4y\frac{1+e^{-y}}{1-e^{-y}}\sum_{n=1}^{\infty}\frac{1}{y^2+\pi^2(2n+1)^2} \\ &= \frac{1+e^{-y}}{1-e^{-y}}\tanh\left(\frac{y}{2}\right) = 1, \end{aligned} \tag{A12}$$

$$P(x,0) = R(x), \tag{A13}$$

$$R(x\to\infty) = \frac{8}{\pi^2}\exp\left(-\pi^2x\right). \tag{A14}$$

Figure 7 Illustrates the function $P(0,y)$ on y parameter [$y=0$ (blue curve), 1 (red), 3 (green), and 10 (cyan)] and the corresponding asymptotics [Eq. (A14)] (shown as dashed lines).

The solution (A8) is exact for any values of parameters $\frac{D\tau}{a_x^2}$ and a_xk_{ex}. It is useful to introduce the diffusion length over the radiation lifetime $L = \sqrt{D\,\tau}$. In the case of bulk

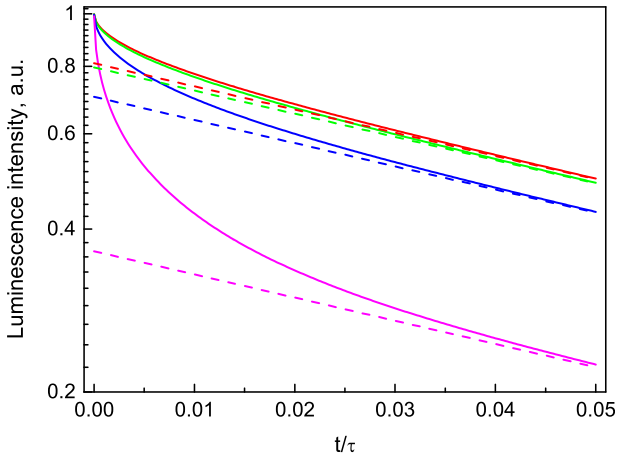

FIG. 7. The function $P(0,y)$ for some values of y parameter [$y=0$ (blue curve), 1 (red), 3 (green), and 10 (cyan)] and the corresponding asymptotics [Eq. (A14)] (shown as dashed lines).

sample, we have to take the limits $a_x k_{ex} \gg 1$, $a_x \gg L$, $a_y \gg L$, $a_z \gg L$. Taking the sums over n_y and n_z and passing to the integral over n_x, we can get the kinetics for the surface quenching for the case of bulk sample

$$I_{lum}(t) = \frac{2a_y a_z}{\pi\tau} I_{ex} k_{ex} \int_0^\infty dx \, \frac{1}{k_{ex}^2 + x^2} e^{-\frac{t}{\tau} - x^2 Dt}$$
$$= \frac{a_y a_z}{\tau} I_{ex} e^{-\frac{t}{\tau} - Dk_{ex}^2 t} \mathrm{Erfc}\left(k_{ex}\sqrt{Dt}\right). \quad \text{(A15)}$$

Integrating this kinetics over time, we can get the known formula for bulk crystal surface quenching

$$\int_0^\infty I_{lum}(t)\, dt = \frac{2a_y a_z}{\pi} I_{ex} k_{ex} \int_0^\infty dx \, \frac{1}{k_{ex}^2 + x^2} \frac{1}{1 + x^2 D\tau}$$
$$= \frac{a_y a_z I_{ex}}{1 + k_{ex}\sqrt{D\tau}} \equiv \frac{a_y a_z I_{ex}}{1 + k_{ex} L}. \quad \text{(A16)}$$

The surface quenching in other limits (nanowire, nanowell) can be also obtained. Here, we are going to discuss mainly the quenching for cubic nanoparticles (the case $a_x = a_y = a_z = a$).

When the nanoparticle size is less than the absorption length, $ak_{ex} \ll 1$, Eq. (A8) can be rewritten as

$$I_{lum}(t) = I_{lum}(0) \exp\left(-\frac{t}{\tau}\right) \left(R\left(\frac{L^2}{a^2}\frac{t}{\tau}\right)\right)^3. \quad \text{(A17)}$$

[1]C. Dujardin, D. Amans, A. Belsky, F. Chaput, G. Ledoux, and A. Pillonnet, IEEE Trans. Nucl. Sci. **57**, 1348 (2010).
[2]V. V. Vistovskyy, A. V. Zhyshkovych, N. E. Mitina, A. S. Zaichenko, A. V. Gektin, A. N. Vasil'ev, and A. S. Voloshinovskii, J. Appl. Phys. **112**, 24325 (2012).
[3]V. V. Vistovskyy, A. V. Zhyshkovych, Y. M. Chornodolskyy, O. S. Myagkota, A. Gloskovskii, A. V. Gektin, A. N. Vasil'ev, P. A. Rodnyi, and A. S. Voloshinovskii, J. Appl. Phys. **114**, 194306 (2013).
[4]T. S. Malyy, V. V. Vistovskyy, Z. A. Khapko, A. S. Pushak, N. E. Mitina, A. S. Zaichenko, A. V. Gektin, and A. S. Voloshinovskii, J. Appl. Phys. **113**, 224305 (2013).
[5]V. Vistovskyy, T. Malyy, A. Pushak, A. Vas'Kiv, A. Shapoval, N. Mitina, A. Gektin, A. Zaichenko, and A. Voloshinovskii, J. Lumin. **145**, 232 (2014).
[6]T. Demkiv, M. Chylii, V. Vistovskyy, A. Zhyshkovych, N. Gloskovska, P. Rodnyi, A. Vasil'ev, A. Gektin, and A. Voloshinovskii, J. Lumin. **190**, 10 (2017).
[7]V. Vistovskyy, N. Mitina, A. Shapoval, T. Malyy, A. Gektin, T. Konstantinova, A. Voloshinovskii, and A. Zaichenko, Opt. Mater. **34**, 2066 (2012).
[8]G. Stryganyuk, D. M. Trots, A. Voloshinovskii, T. Shalapska, V. Zakordonskiy, V. Vistovskyy, M. Pidzyrailo, and G. Zimmerer, J. Lumin. **128**, 355 (2008).
[9]A. N. Belsky and J. C. Krupa, Displays **19**, 185 (1999).
[10]G. Zimmerer, Radiat. Meas. **42**, 859 (2007).
[11]J. Becker, M. Kirm, V. N. Kolobanov, and V. N. Makhov, Electrochem. Soc. Proc. **98–25**, 415 (1998).
[12]Y. M. Aleksandrov, V. N. Makhov, T. I. Syrejshchikova, and M. N. Yakimenko, Nucl. Instrum. Methods Phys. Res., Sect. A **261**, 158 (1987).
[13]P. A. Rodnyi, N. N. Ershov, N. G. Zakharov *et al.*, Opt. Spectrosk. **53**, 89 (1982).
[14]G. W. Rubloff, Phys. Rev. B **5**, 662 (1972).
[15]A. F. Latypov *et al.*, see http://www.math.nsc.ru/conference/ipmp07/abstracts/Section3/LatypovAF_rus.doc for in *International Conference* "Inverse and incorrect problems of mathematical physics," dedicated to the 75th Anniversary of Academician M. M. Lavrent'ev, 20–25 August 2007, Novosibirsk, Russia.